Computational Fluid Dynamics Study of Flow and Aerosol Concentration Patterns in a Ribbed Smoked Sheet Rubber Factory

Article *in* Particulate Science And Technology · May 2012

DOI: 10.1080/02726351.2011.562277

CITATIONS
0

READS
176

2 authors:

Lasman Parulian Purba
Universitas Katolik Darma Cendika
4 PUBLICATIONS **17** CITATIONS

SEE PROFILE

Perapong Tekasakul
Prince of Songkla University
52 PUBLICATIONS **586** CITATIONS

SEE PROFILE

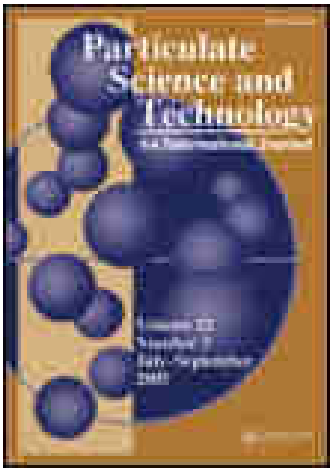

Particulate Science and Technology: An International Journal

Publication details, including instructions for authors and subscription information:
http://www.tandfonline.com/loi/upst20

Computational Fluid Dynamics Study of Flow and Aerosol Concentration Patterns in a Ribbed Smoked Sheet Rubber Factory

Lasman P. Purba [a] & Perapong Tekasakul [b c]

[a] Department of Industrial Engineering, School of Creative Industry , Pelita Harapan University , Surabaya , Indonesia

[b] Energy Technology Research Center, and Department of Mechanical Engineering, Faculty of Engineering , Prince of Songkla University , Songkhla , Thailand

[c] National Center of Excellence for Environmental and Hazardous Waste Management (EHWM)-Southern Consortium Universities at Prince of Songkla University , Songkhla , Thailand

Accepted author version posted online: 21 Nov 2011.Published online: 03 May 2012.

To cite this article: Lasman P. Purba & Perapong Tekasakul (2012) Computational Fluid Dynamics Study of Flow and Aerosol Concentration Patterns in a Ribbed Smoked Sheet Rubber Factory, Particulate Science and Technology: An International Journal, 30:3, 220-237, DOI: 10.1080/02726351.2011.562277

To link to this article: http://dx.doi.org/10.1080/02726351.2011.562277

Particulate Science and Technology, 30: 220–237, 2012

ISSN: 0272-6351 print/1548-0046 online
DOI: 10.1080/02726351.2011.562277

Computational Fluid Dynamics Study of Flow and Aerosol Concentration Patterns in a Ribbed Smoked Sheet Rubber Factory

LASMAN P. PURBA[1] AND
PERAPONG TEKASAKUL[2,3]

[1]Department of Industrial Engineering, School of Creative Industry, Pelita Harapan University, Surabaya, Indonesia
[2]Energy Technology Research Center, and Department of Mechanical Engineering, Faculty of Engineering, Prince of Songkla University, Songkhla, Thailand
[3]National Center of Excellence for Environmental and Hazardous Waste Management (EHWM)-Southern Consortium Universities at Prince of Songkla University, Songkhla, Thailand

A computational fluid dynamics (CFD) method was used to investigate velocity, temperature, particles trajectories, and aerosol concentration in a natural ribbed smoked sheet rubber factory. A model to improve the smoke aerosol particle ventilation was proposed. The simulation was performed using turbulent free convection flows where the Rayleigh number was between 5.3838×10^{10} and 33.2003×10^{10}. A total of 2,159,347 mesh volumes were applied to the entire ribbed smoked sheet rubber cooperative. Results from the CFD simulation and experiment showed positive results. The air containing smoke particles moved naturally from ventilating lids of the smoke room to the roof. The smoke particles followed the airflow fields at the junction of the roof and traveled to workplace areas. Results show that the thick cloud of smoke particles remained in the workplace after traveling for more than 200 m. Particle concentration was high in the area above the ceiling and lower along the elevation in a downward direction. This is potentially harmful to the employees who work in the factory for long periods of time. Modification of the roof to include a ridge vent showed considerable improvement in ventilation, which largely decreased the aerosol particle concentration inside the factory.

Keywords CFD, free convection, natural rubber, smoke particle, ventilation

This research was financially supported by the NRCT-JSPS Joint Research Program (National Research Council of Thailand–Japan Society for the Promotion of Science Joint Research Program). Appreciation is also extended to the Saikao Cooperative, which is located in Tambon Toongwang, Muang District, Songkhla Province, Thailand, for allowing researchers to have access to the facility.

Address correspondence to Perapong Tekasakul, Energy Technology Research Center, and Department of Mechanical Engineering, Faculty of Engineering, Prince of Songkla University, Hat Yai, Songkhla 90112, Thailand. E-mail: perapong.t@psu.ac.th

Introduction

Natural rubber (*Hevea brasiliensis*) is one of the major plants in the global economy. Products made from pure mixtures of natural rubber and other materials include automotive tires, medical gloves, condoms, toys, and industrial parts (Doo-ngam et al. 2007; Promtong and Tekasakul 2007; Chomanee et al. 2009). One of the main midstream products manufactured before shipping to downstream industries is ribbed smoked sheet (RSS) rubber. Currently in Thailand, there are about 500 rubber cooperatives, and production of ribbed smoked sheets has shifted from large factories to small-scale community-based cooperatives. There are two cooperative models, the 1994 and 1995 models. These two models differ in the size of smoke rooms and, hence, the capacity for production of rubber sheets. In the 1995 model, the size of the rubber sheet smoke room is 5.0 m (width) $\times$ 4.0 m (height) $\times$ 6.0 m (depth), which is double the size of the smoke room in the 1994 model (Choosong et al. 2010).

During ribbed smoked sheet production, rubber-wood is burned to supply heat and smoke to the rubber sheets in a smoke room (Promtong and Tekasakul 2007; Tekasakul and Promtong 2008). Wood burning generates a large portion of fine smoke aerosol particles, which contain harmful chemicals such as polycyclic aromatic hydrocarbons or PAHs (Chomanee et al. 2009). This is potentially detrimental to the health of the factory workers because such particles are able to flow into the workplace area of the RSS rubber cooperative.

Improvement of airflow in factories is a necessary process in order to reduce health risks for workers due to exposure to these smoke particles. Recent particle concentration data in workplace areas has been obtained (Choosong et al. 2007; Choosong et al. 2010). However, no studies of airflow have been conducted. Therefore, it is necessary to study the airflow, particle trajectories, and particle concentration inside workplace areas of RSS rubber cooperative. This type of research may lead to appropriate methods of controlling and ventilating the particles.

The present research study began with a simulation of velocity and temperature distributions and particle concentration, as well as smoke particle trajectories, inside of a ribbed smoked sheet rubber cooperative. The computational fluid dynamics (CFD) technique was used to perform the simulation of airflow and aerosol transport in the current smoking cooperative. Experimental verification of particle concentration was performed. The CFD simulation allowed for investigation of means to improve airflow inside the cooperative.

Problem Description

Model Geometry and Experiments

Experiments were conducted in a building within the 1995 Saikao RSS cooperative model, located in Muang district of Songkhla province, Thailand. The geometry of the cooperative factory building is shown in Figure 1. Four RSS smoke rooms (5.0 m $\times$ 4.0 m $\times$ 6.0 m) are located on one side, while the opposite side is mostly open space. Two 0.6 m $\times$ 0.6 m square ventilating lids are installed on the ceiling of each smoke room. In Figure 1, only two ventilating lids, labeled B1 and B2, in room B are shown because the experiments and simulations were conducted on a day when only room B was in operation. Locations of rooms A, C, and D are shown in detail in Figure 2.

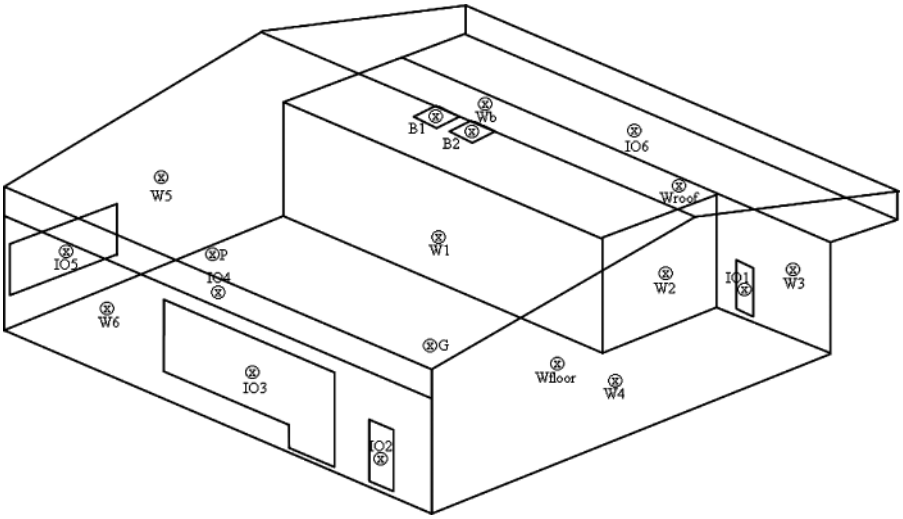

Figure 1. Positions of velocity and temperature measurements in the ribbed smoked sheet rubber cooperative.

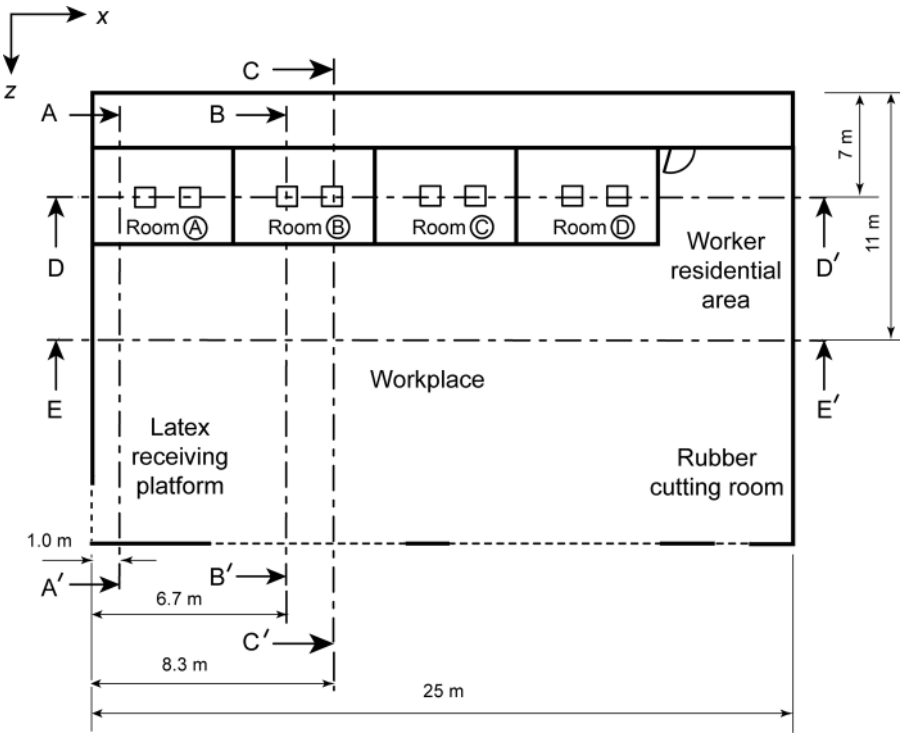

Figure 2. Top view of the cooperative layout describing planes to display the velocity and temperature distributions.

Velocity and temperature measurement probes were installed in the positions shown in Figure 1. IO1 and IO2 are the entrance and exit openings located on the rear and front sides of the cooperative, respectively. IO3 is the opening above the front wall designed for ventilation. It was divided into 16 equal partitions for velocity and temperature measurement purposes. Measurement positions were located at the center of each partition. IO4 is the opening above IO3 and below the roof edge designed for ventilation purposes, and it is divided into five partitions. IO5 was the entrance to the cooperative located 1.3 m above the workplace ground, and it is used for cooperative members to deliver the rubber latex. IO6 was the ventilation opening on the rear side, and it was on the same level as the ceiling of the rubber smoke rooms. It was divided into five equally spaced partitions for measurement, as well. Walls inside the cooperative were divided into six sections (W1 to W6), which are also shown in Figure 1. Other solid boundaries included the roof (Wroof), the smoke room ceiling (Wb), and the floor (Wfloor).

The velocity of the air was measured by hot-wire type anemometers (Airflow Instrumentation, TA400T, 0–2 m/s, and Testo, 405-V1, 0–10 m/s). Air temperature was measured using type-K thermocouples and recorded with a data logger (DataTaker, DT605) at three-second intervals to ensure about 3 h of continuous measurement. Then, averages were found for all data and used as boundary conditions for the simulation.

Smoke particle concentration in the workplace area was measured at location P, as illustrated in Figure 1. It was measured at three elevations from the ground (P1 at 1.5 m, P2 at 3.0 m, and P3 at 4.5 m) to investigate the height dependence of the concentration. A self-made sampling system, consisting of a vacuum cleaner as a sampling pump, was used to take samples. Three filter holders and corresponding orifice meters were used to measure the flow rate, which was controlled by separate valves. Samples were taken at 150 L min^{-1} for 90 min. HEPA-type filters (Cambridge Filter, 110-mm diameter) were used for aerosol collection. The filters were conditioned in a controlled environment (25°C, 50% RH) for 48 h prior to and after samples were taken. The mass of the collected particles was then used to calculate particle concentration. Samples were also taken from ventilating lids in the rubber sheet smoke room. The average concentration from these lids was used as a boundary condition for evaluation of particle concentration distribution in the factory.

Firewood (rubber-wood) of known mass was fed to the burner. Samples of firewood were used to determine the moisture content on a dry basis by drying them in a laboratory oven at 105°C until completely dry. In this experiment, there were 2,600 pieces of RSS produced, and the fuel (rubber-wood) used in each room weighed 2,100 kg.

Boundary Conditions

Velocity and temperature data from measurements used for boundary conditions in CFD are presented in Table 1. The data at locations IO3, IO4, and IO6 show average values from all partitions. Moreover, values from each measuring point represent average values from 10 measurements. Static pressure boundary condition was used to represent the system surroundings and was at a constant value of zero gauge pressure with an ambient temperature of 33.2°C.

At the ventilating lid exits, the average velocity of every particle was 1.03 m/s, the temperature was 48.6°C, and the average aerosol concentration was

Table 1. Average values of measured velocity and temperature used as boundary conditions

Location	Velocity (m/s)	Temperature (°C)
B1	1.03	48.7
B2	1.02	48.5
IO1	0.79	31.5
IO2	0.49	31.6
IO3	0.32	32.3
IO4	0.35	33.9
IO5	0.35	31.4
IO6	0.01	35.0
W1	0.0	47.6
W2	0.0	44.1
W3	0.0	33.9
W4	0.0	42.2
W5	0.0	32.1
W6	0.0	32.1
Wb	0.0	36.4
Wfloor	0.0	32.5
Wroof	0.0	39.8

$4.178\,\mathrm{mg/m^3}$. This resulted in an aerosol mass flow rate of $1.5416 \times 10^{-6}\,\mathrm{kg/s}$. The average aerosol concentration was used as a boundary condition for the simulation.

Simulation Approach

The present research study involves a simulation of airflow, particle trajectories, and particle concentration in a workplace area of a ribbed smoked sheet rubber cooperative. Therefore, theoretical background of relevant fluid flow and aerosol particle motion is necessary and will be presented in the following section.

The numerical solution of fluid flow and other related processes can begin with the laws governing these processes, which are expressed in mathematical forms, generally in terms of differential equations (Patankar 1980). The individual equations describe certain conservation principles and employ certain physical properties as dependent variables. The dependent variables are usually specific extensive properties, that is, properties expressed on a unit-mass basis. Examples include mass fractions, velocity (momentum per unit mass), specific enthalpy, and particle concentration per unit mass.

Flow Equations

The continuity equation describing mass conservation for a steady incompressible flow used in this work can be written as:

$$\frac{\partial}{\partial x_i}(\rho \bar{u}_i) = 0. \tag{1}$$

For the case of the RSS cooperative, the flow is naturally induced. The differential equations for the conservation of momentum, or the Navier-Stokes Equations,

take the following form:

$$\frac{\partial}{\partial x_i}\left(\rho\overline{u_j u_i}\right) = -\frac{\partial \bar{p}}{\partial x_i} + \frac{\partial}{\partial x_j}\left[\mu\left(\frac{\partial \overline{u}_i}{\partial x_j} + \frac{\partial \overline{u}_j}{\partial x_i}\right) - \rho\overline{u_i' u_j'}\right] - \rho g_i \beta\left(\overline{T} - \overline{T}_{ref}\right). \quad (2)$$

The energy equation can be written as:

$$\frac{\partial}{\partial x_i}\left(\rho\overline{u_i T}\right) = \frac{\partial}{\partial x_i}\left[\frac{\mu}{\mathrm{Pr}}\frac{\partial \overline{T}}{\partial x_i} - \rho\overline{u_j' T'}\right], \quad (3)$$

where i is the directions (x, y, z in Cartesian coordinates), $\bar{u}$ is the mean of the velocity components (u, v, w), $\overline{u_i'}$ is the velocity fluctuation, $\bar{p}$ is the pressure, μ is the fluid viscosity, and Pr is the Prandtl number. Here, x_i is the coordinate axis (x, y, z), ρ is the fluid density, g_i is the gravitational acceleration vector, and β is the thermal expansion coefficient. The Boussinesq approximation is employed in the last term of Equation (2). Here, T_{ref} is the reference temperature (the system surrounding temperature is used in this work), $\overline{T}$ and $\overline{T'}$ are the mean temperature and temperature fluctuation, respectively. The term $-\overline{\rho u_i' u_j'}$ is called the Reynolds stress (τ_{ij}) and $-\overline{\rho u_i' T'}$ is the diffusion term for the enthalpy. The determination of these terms requires extra equations. Turbulence models are used to determine correlations of these terms with the mean flow field.

The flow in a workplace of the RSS factory is generally natural. Since the Rayleigh number, $Ra = g\beta(T_s - T_\infty)H^3/\nu\alpha$, lied between 5.3838×10^{10} to 33.2003×10^{10} (for ΔT between 1.2 to 7.4°C) in this experiment, the flow became turbulent. The most widely used standard $k-\varepsilon$ turbulent model was used in this simulation. It is a semi-empirical model, and the derivation of the model equations relies on phenomenological considerations and empiricism. Details of the model are given by Promtong and Tekasakul (2007).

In the present study, Equations (1)–(3) were solved in order to obtain velocity and temperature patterns in the factory.

Aerosol Concentration and Motion

Distributions of smoke aerosol concentration in the factory were calculated by assuming that the smoke particle-laden air was a fluid with the density of air. This assumption is accurate in this case because of the small particle size, mass median aerodynamic diameter (MMAD) ranging from 0.85 to 0.95 μm (Kalasee et al. 2003; Choosong et al. 2010). Therefore, it was possible to neglect the influence of gravity and inertia.

Diffusion of dust was calculated from the convective diffusion equation (Kanaoka et al. 2006):

$$\frac{\partial}{\partial t}(\rho X) + \frac{\partial}{\partial x_i}(\rho u_i X) = -\frac{\partial J_i}{\partial x_i} \quad (4)$$

where X is the mass fraction, u_i is the air velocity, ρ is the air density, and J_i is the local current for i-component defined as:

$$J_i = -\left(\rho D + \frac{\mu_t}{Sc}\right)\frac{\partial X}{\partial x_i}. \quad (5)$$

In this equation, D is the diffusion coefficient, μ_t is the turbulent viscosity, and Sc is the Schmidt number equal to 0.7.

By assuming particle flow is a continuum, aerosol particle trajectory can be found by representing it in a discrete phase. The trajectory of a discrete phase of particles is predicted by integrating the force balance on the particle, which is written in a Lagrangian frame of reference (Tian et al. 2007). This force balance equates the particle inertia with the forces acting on the particle. It can be written, for the x-direction in the Cartesian coordinates, as (Chow and Yin 2006):

$$\frac{du_{pi}}{dt} = F_{Di}(u_i - u_{pi}) + \frac{g_i(\rho_p - \rho)}{\rho_p}. \tag{6}$$

In this equation, u_p is the particle velocity, ρ_p is the density of the particle, d_p is the particle diameter, and F_D is the drag force per unit particle mass given by

$$F_{Di} = \frac{18\,\mu}{\rho_p d_p^2}\frac{C_D \mathrm{Re}}{24}, \tag{7}$$

where Re is the relative Reynolds number, defined as

$$\mathrm{Re} \equiv \frac{\rho d_p |u_{pi} - u_i|}{\mu}. \tag{8}$$

The drag coefficient, C_D, is described by (Haider and Levenspiel 1989)

$$C_D = \frac{24}{\mathrm{Re}}\left(1 + b_1 \mathrm{Re}^{b_2}\right) + \frac{b_3 \mathrm{Re}}{b_4 + \mathrm{Re}}, \tag{9}$$

where

$$\begin{aligned} b_1 &= \exp(2.3288 - 6.4581\varphi + 2.4486\varphi^2) \\ b_2 &= 0.0964 + 0.5565\varphi \\ b_3 &= \exp(4.905 - 13.8944\varphi + 18.4222\varphi^2 - 10.2599\varphi^3) \\ b_4 &= \exp(1.4681 + 12.2584\varphi - 20.7322\varphi^2 + 15.8855\varphi^3). \end{aligned} \tag{10}$$

The shape factor, φ, is defined as

$$\varphi = \frac{S_e}{S}, \tag{11}$$

where S_e is the surface area of a sphere having the same volume as the particle, and S is the actual surface area of the particle.

Calculation Technique

CFD is a universal tool to predict indoor airflows, and it has been used since the early 1970s. It has gained popularity among researchers in the field of fluid dynamics in the last few decades as a result of advancement in computing power (Einberg

2005; Hussein et al. 2005; Zang and Chen 2006; Sohn et al. 2007). CFD has been primarily used to simulate air movement and contaminant dispersion (Hubert et al. 2004; Tian et al. 2007). The application of CFD includes internal environments with large open spaces, such as atriums, museum, theaters, and coliseums. Additionally, it has been used to study distributions of dust flow and concentration in a mountain tunnel (Kanaoka et al 2006).

The CFD is a mathematical modeling procedure, whereby fluid parameters of velocity, temperature, pressure, turbulence, and contaminant concentrations are calculated by solving the governing partial differential equations for fluid flow, heat transfer, and molecular diffusion Equations ((1)–(4) and (6)). These differential equations describe a three-dimensional viscous fluid flow field. Due to the nonlinearity of these equations, they generally cannot be solved analytically. The CFD approach is used to transform these differential equations into a set of discrete algebraic equations, and an iterative procedure is used to solve them.

In the present study, CFD simulations were performed on a desktop computer (Pentium 4, CPU 2.79 GHz and 2 MB of RAM). GAMBIT 2.2 was used to generate the mesh, and the calculation was achieved with FLUENT 6.3. The tetrahedral/hybrid (TGrid) element mesh scheme having a mesh size of 0.2 m, and 2,159,347 total mesh volumes of this size were generated. The convergence criteria were set at 10^{-3} for continuity-, momentum- and standard $k-\varepsilon$ model- equations, and 10^{-6} for energy equation. A control-volume-based technique, the finite volume method, was used to represent discretization.

Results and Discussion

Current Model Configuration: Validation

1. Computation and Representations

Velocity vectors of flow pattern in the cooperative are displayed in five planes, as shown in Figure 2, and they demonstrate the flow behavior inside the entire domain. Planes $A-A'$, $B-B'$, and $C-C'$ are the Y-Z planes cut along the X axis at X = 1.0, 6.7, and 8.3 m, respectively. Plane $A-A'$ is near the left wall of the factory, and it includes the sampling points P1, P2, and P3. Plane $B-B'$ is cut through the center of the ventilating lid B1, while plane $C-C'$ is cut through the center of the ventilating lid B2. Results in these planes should exhibit the influence of smoke particles released from the smoke room. Planes $D-D'$ and $E-E'$ are the X-Y planes cut along Z-axis at Z = 7.0 and 11.0 m, respectively. Plane $D-D'$ is cut through the centers of all ventilating lids to show the influence of smoke particles in an additional plane. Plane $E-E'$ is cut through the center of the factory, and it is used as a representative example of the workplace.

The results from all five planes demonstrate the whole flow patterns, temperature distributions, and particle concentration contours in the ribbed smoked sheet rubber cooperative.

2. Velocity Fields

The velocity of air in the present ribbed smoked sheet rubber cooperative is displayed in Figures 3a–3e. The flow under investigation was assumed to be steady. Air velocity magnitudes at the ventilating lids B1 and B2 were highest (1.02 and 1.03 m/s) and were used as boundary conditions.

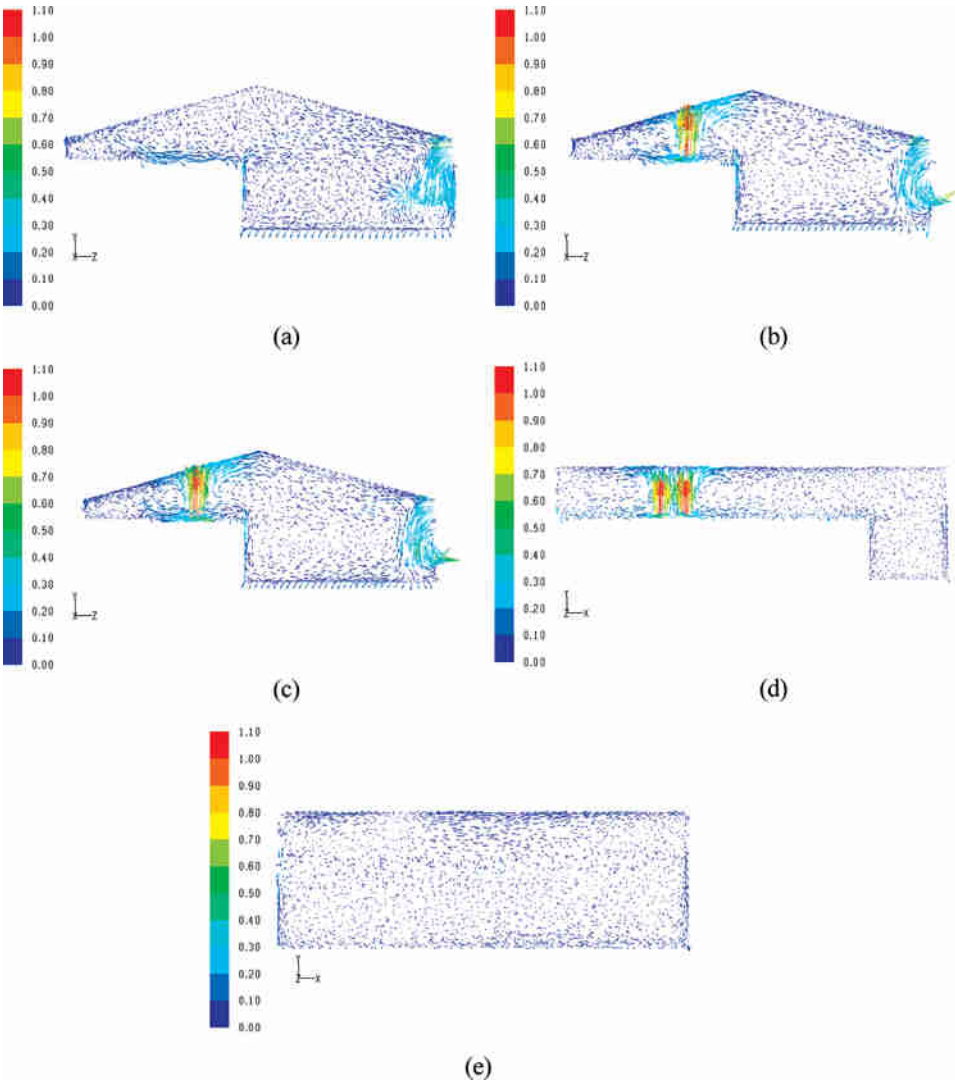

Figure 3. The velocity of air in the present ribbed smoked sheet rubber cooperative (m/s) at planes (a) $A - A'$, (b) $B - B'$, (c) $C - C'$, (d) $D - D'$, and (e) $E - E'$. (Figure available in color online.)

Results show that air from the ventilation opening on the rear side behind the smoke rooms (IO6) moved up to the rubber smoke room ceiling and then upward toward the roof. The air combined with exhaust from the ventilating lid and airflow near the floor. This combination of air and exhaust moved upward and caused swirls due to the buoyancy effect (Figures 3a–3c). When it reached the roof, the flow spread radially throughout the factory (Figures 3b–3d). During this time, flow from the opening window IO4 was combined with the flow from the opening window at the entrance on the second floor (IO5) and exited the factory through the same opening at the lower part (IO3), as shown in Figures 3a–3c. The magnitudes of velocity at

the right side of planes B – B′ and C – C′ (Figures 3b and 3c ranged from 0.03 to 0.12 m/s, and at the bottom part of the factory (bottom-left side of the figure) the velocity was as low as 0.07–0.10 m/s.

The airflow pattern in plane D – *D*′ (Figure 3d) shows that on the left side, the flow around the ceiling of the rubber smoke room and roof of the cooperative was influenced by the flow from the opening at the bottom-left side (IO6), which caused a swirl that moved in a counter-clockwise direction. On the right side, the flow around the ceiling of the ventilating lids and the roof of the cooperative moved in the opposite direction.

In the center of the cooperative, the velocity was nonuniform, as shown in Figure 3e. The flows from the ventilating lids influenced the flow in the area above the ceiling. However, the magnitudes of the velocity were low. The maximum velocity magnitude was approximately 0.19 m/s in the area around one-third of the height at the left side from the roof. Most of the flow circulated inside the workplace without exiting. This indicates improper ventilation of air and smoke inside the workplace. Therefore, it is clear that an improvement of ventilation is necessary to enhance the air quality in the workplace area.

Comparisons of velocity between the simulation and experiment at various locations are shown in Figure 4. Error of velocity between measurement and simulation at location P was high because workers often delivered rubber latex at the opening around the second floor (IO5) near point P. This may have caused disturbances to the airflow when measurements were performed. Errors in measurement were high at a few other locations because they were measured in real situations and included many uncontrollable factors. In general, results show sufficiently positive agreement with an average error of less than 22%.

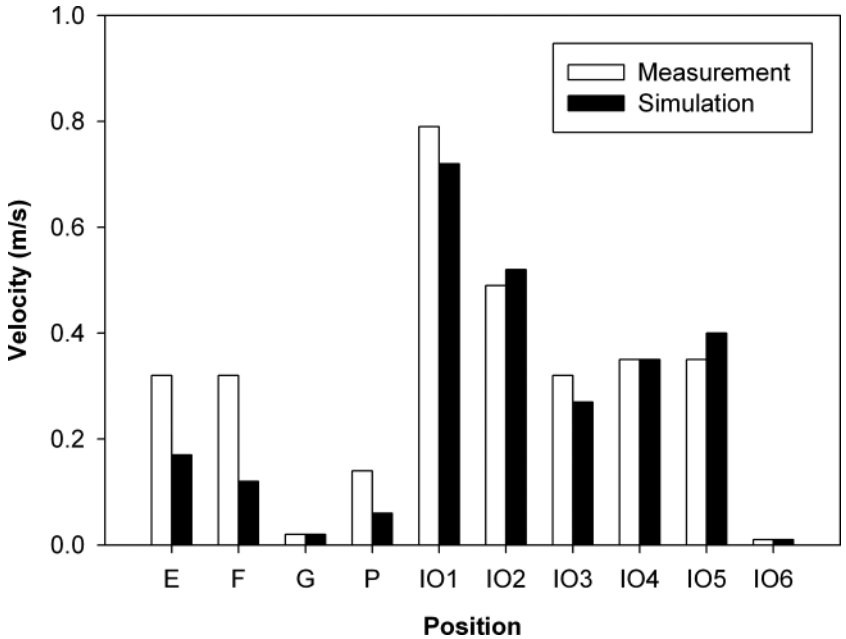

Figure 4. Comparison of velocity from measurement and simulation.

3. Temperature

Air temperature patterns in the present ribbed smoked sheet rubber cooperative are displayed in Figures 5a–5e. Due to the buoyancy effect resulting from the exhaust of hot gas coming from the ventilating lids, the temperature above the ventilating lids was the highest and consistently higher than 40°C. Heat ventilation from the roof area was limited because no openings were present. Temperatures near all openings were low because of the inlet flowing of ambient air. The area near the front doors of the smoke rooms experienced a slight rise in temperature due to the heat transfer from the smoke rooms to the workplace area.

Overall, the lowest temperature was 31.4°C, which occurred at the entrance of the cooperative where air flows freely from the outdoor to the indoor work

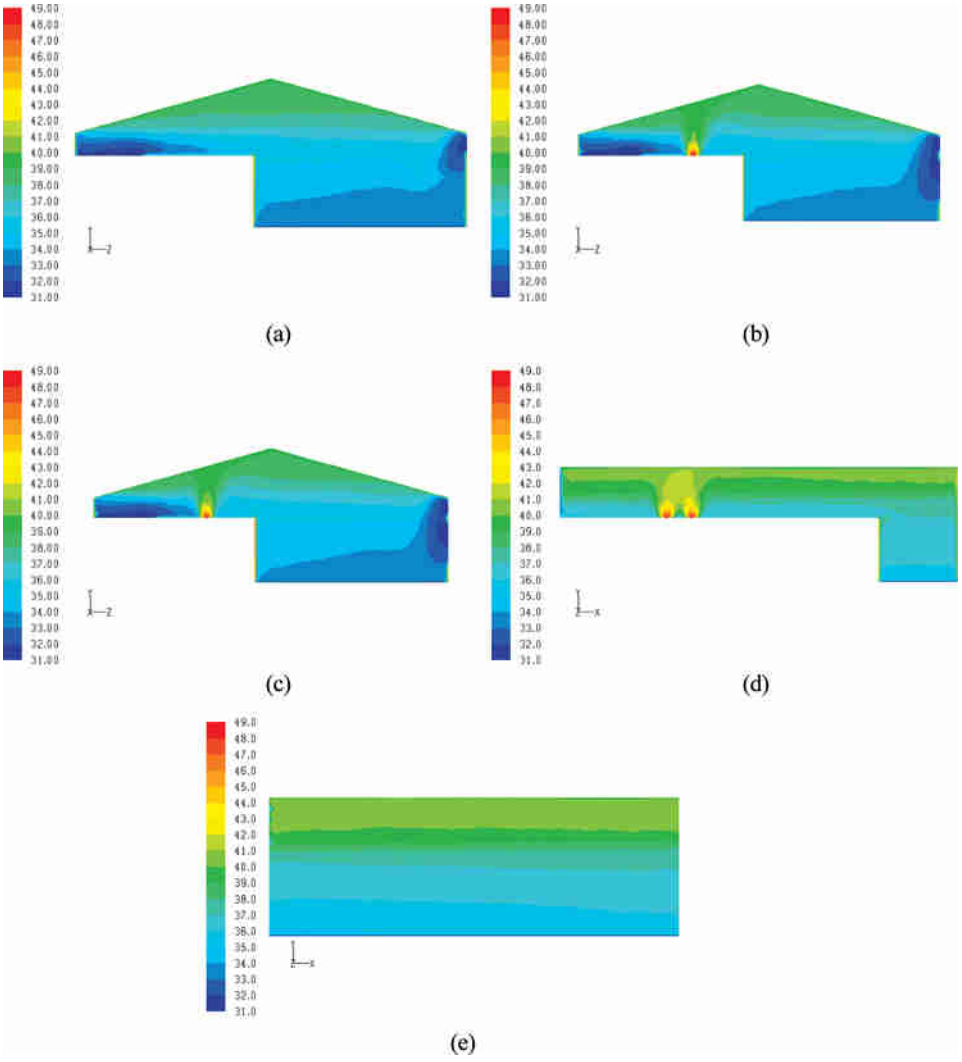

Figure 5. The temperature of air in the present ribbed smoked sheet rubber cooperative (°C) at planes (a) $A - A'$, (b) $B - B'$, (c) $C - C'$, (d) $D - D'$, and (e) $E - E'$. (Figure available in color online.)

environment. As expected, the highest temperature was found near the ventilating lids at 48.7°C.

Comparisons of temperatures between the simulation and experiment at various locations are shown in Figure 6. The results show a positive agreement between the measurement and simulation values with less than 6% error, indicating a proper simulation scheme.

4. Particle Trajectory

The trajectories of particles released from the surfaces of the opened ventilating lids B1 and B2 are shown in Figure 7. The particles were released normal to boundaries and would deposit if they collided with the walls (coefficient of restitution was zero). There were 18 sampled particles released; nine particles from each ventilating lid. The particle diameter was assumed to be a uniform 1.0 μm in length because smoke particles under consideration were the result of burned rubber-wood. The resulting smoke particle mass median aerodynamic diameter (MMAD) was found to be near 1.0 μm (Kalasee et al. 2003; Choosong et al. 2010).

The smoke particles followed the airflow fields where some of them left the junction of the roof, while some were deposited onto the walls. The particles seemed to be congested near the roof area before they were vented out of the cooperative. One particle escaped via the entrance to the cooperative (IO5) on the left side, while the other 17 particles were still contained inside of the RSS cooperative for a specific number of steps during the simulation after an average traveling distance of about 200 m. This indicates a long residence time for the particles in the cooperative, which is potentially harmful for employees working in this area.

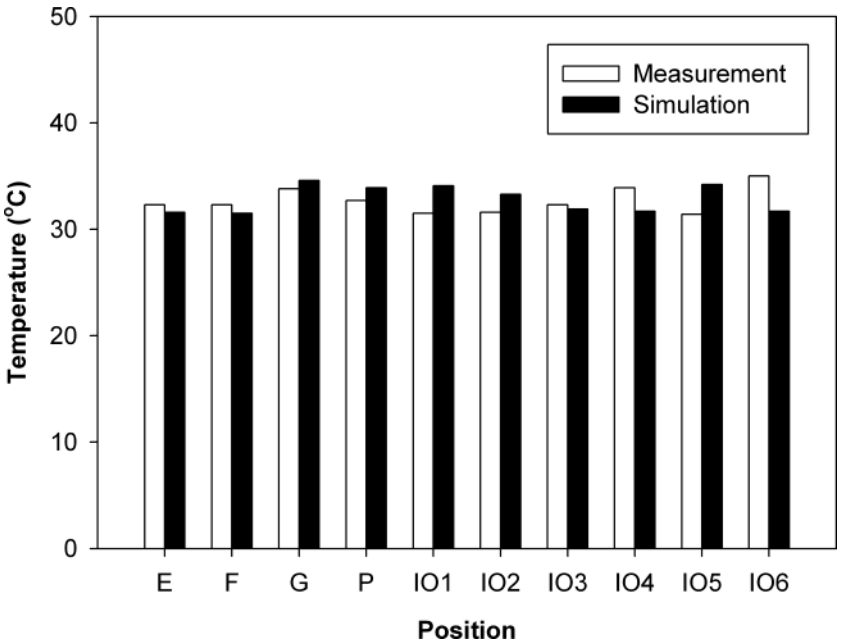

Figure 6. Comparison of temperature from measurement and simulation.

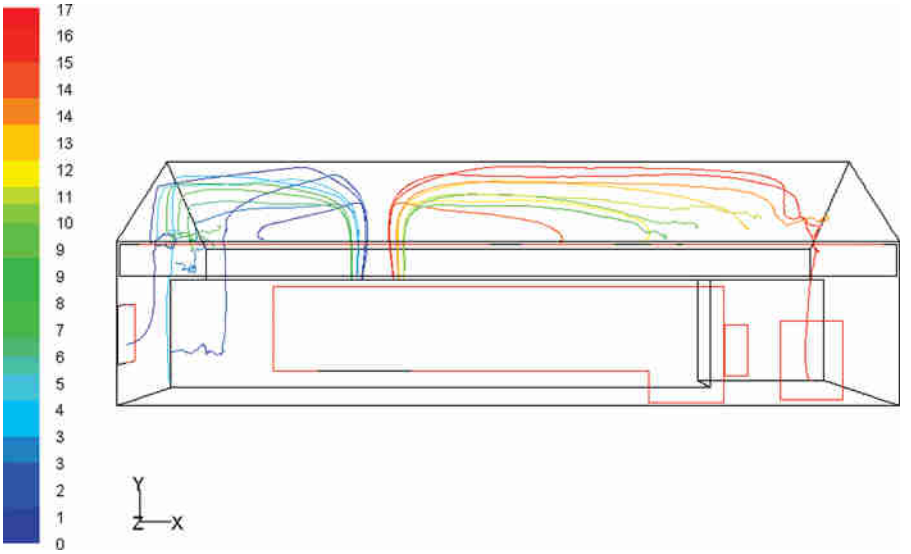

Figure 7. Trajectories of smoke particles released from B1 and B2 (average traveling distance of about 200 m). (Figure available in color online.)

5. Particle Concentration

The particle concentration in the present ribbed smoked sheet rubber cooperative is displayed in Figures 8a–8e. Simulation results of contours of particle concentrations show that the areas nearest to the ventilating lids contained the highest particle concentration, as these were the sources of aerosol particles at the workplace. The particles moved up to the roof following air streamlines, as discussed in the preceding section. The concentration was reduced along a downward direction of elevation. Although the concentration at the working elevation was not very high, the particles were congested in the area above the workplace because their residence times were very long. If all the smoke rooms were in use, it is possible that the concentration of particles could become drastically high at the working elevation. Hence, proper ventilation of these smoke particles is required.

Comparisons between the simulation and measurement results of particle concentration were conducted at three positions (P1, P2, and P3), as shown in Figure 9. Agreement of the simulation and measurement results are acceptable with an average error of less than 31%, especially considering the difficulty in the measurement with uncontrollable conditions. It is concluded that particle concentration increases along an increasing elevation in the workplace area. Concentration above the ceiling of the smoke rooms (P3: 4.5 m) was more than three times as high as it was at the working elevation (P1; 1.5 m). This is in accordance with the particle trajectories that were discussed previously.

Proposed Improvement Model

There are many alternative possibilities for improving ventilation of smoke particles in the RSS rubber cooperative. Since the particles were congested in the roof area because there was insufficient ventilation, the roof was modified to be a ridge-vent

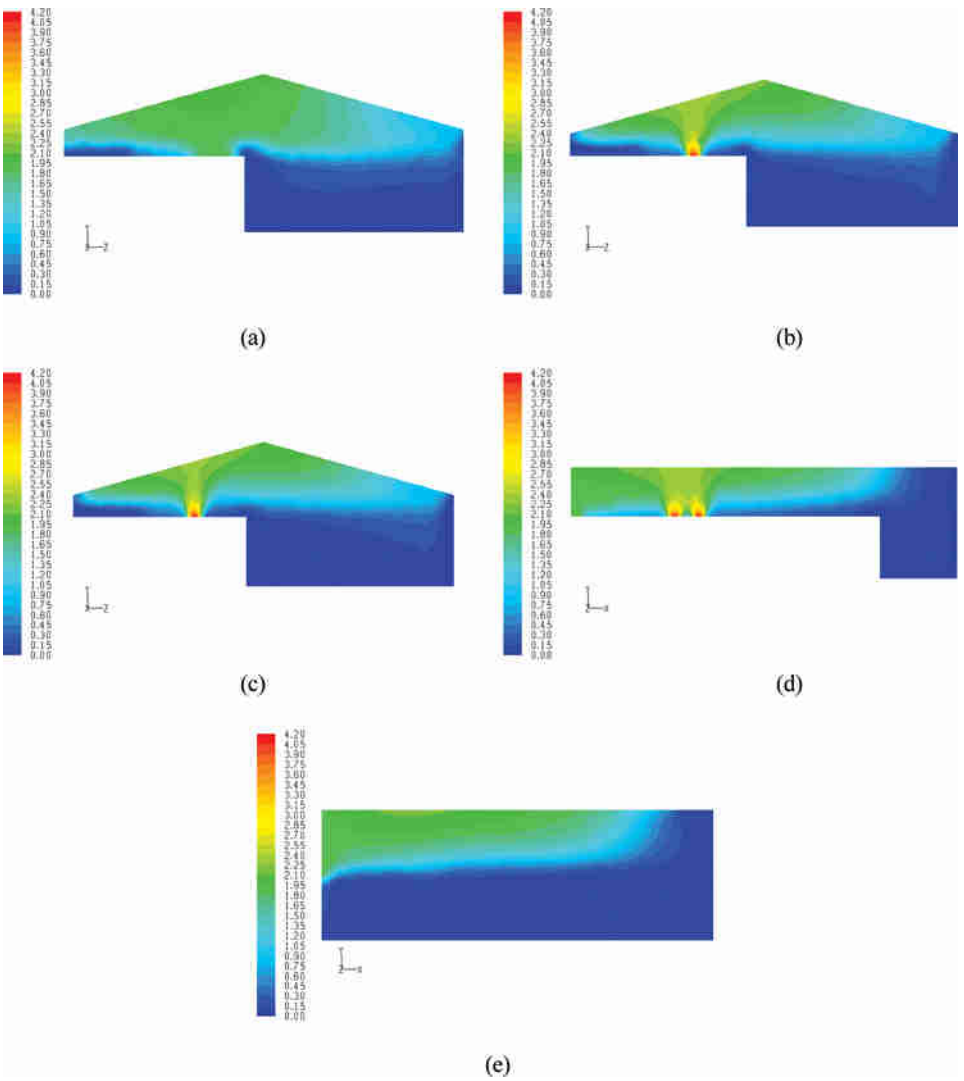

Figure 8. Contours of particle-concentrations (mg/m^3) at planes (a) $A-A'$, (b) $B-B'$, (c) $C-C'$, (d) $D-D'$, and (e) $E-E'$. (Figure available in color online.)

type in order to create natural ventilation. This site was used to study the effects of ventilation improvement.

The configuration considered in this work is shown in Figure 10, and the dimensions varied are shown in Table 2. Variations of the dimensions a, b, and c were conducted in four cases to compare ventilation capabilities. The dimension a is the horizontal span of the improved roof, b is the dimension of the opening height (vertical span), and c is the dimension of span according to variations of a and b. Positions L, M, and N were the monitoring points for velocity, temperature, and aerosol concentration. These values were used during discussion of ventilation improvement.

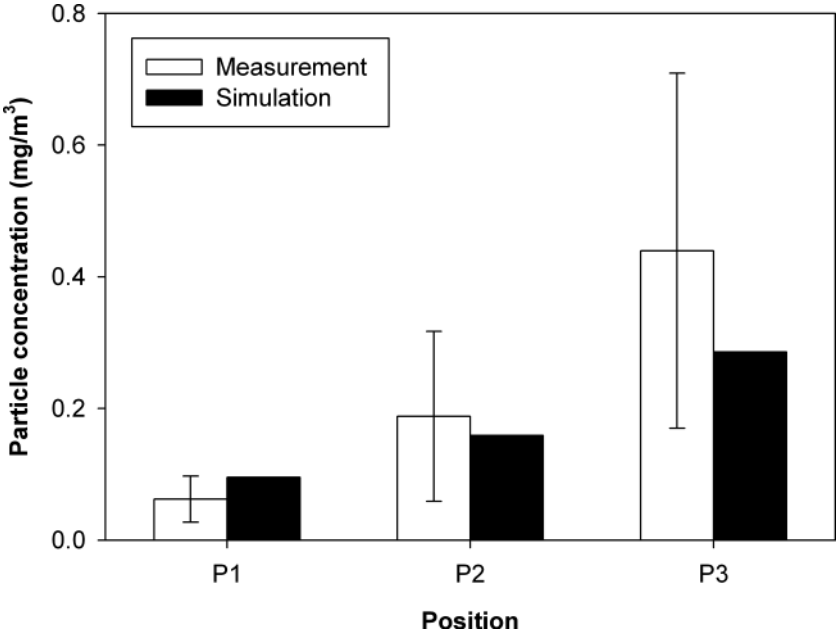

Figure 9. Comparison of particle distribution from measurement and simulation.

Comparisons of velocity, temperature, and aerosol concentrations at several positions are summarized in Table 3. The velocity representatives after improvement were based on velocities at points *L*, *M*, and *N*. Cases 1 and 4 resulted in the highest values shown, while temperatures at point *L* were practically unchanged for all cases. However, the concentrations of aerosol in the workplace area (positions P1, P2, and P3) were lowest during Case 1, although the concentration at point *L* varied. This was due to the location of the largest openings in the improved rooftop. At these values, the workplace smoke particle contamination was reduced significantly and brought to safe levels; however, the openings can be made larger in order to further reduce the aerosol concentrations.

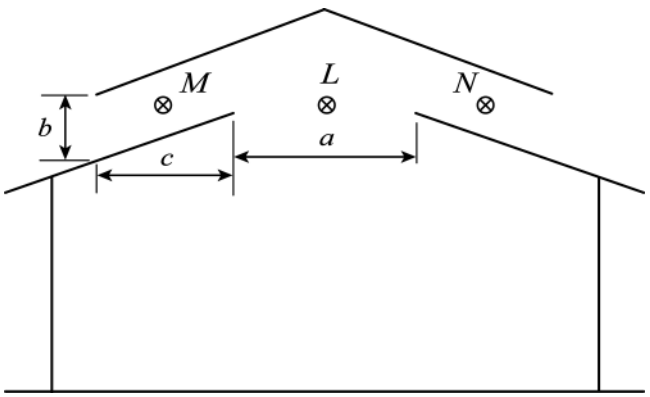

Figure 10. Configuration and dimensions of the improved cooperative.

Table 2. Parameters of dimensions varied in the ventilation improvement simulation

Case	*a* (m)	*b* (m)	*c* (m)
1	3.0	1.0	3.6
2	3.0	0.5	1.8
3	2.0	1.0	3.6
4	2.0	0.5	1.8

Table 3. Comparison of velocity, temperature and aerosol concentration for all ridge-vent cases

	Velocity (m/s)			Temperature (°C)	Concentration (mg/m^3)			
Case	*L*	*M*	*N*	*L*	*L*	P1	P2	P3
1	0.17	0.20	0.38	39.5	1.463	0.024	0.023	0.060
2	0.07	0.00	0.09	44.1	1.681	0.074	0.493	0.654
3	0.16	0.06	0.12	40.3	0.976	0.062	0.080	0.294
4	0.18	0.35	0.38	40.3	1.760	0.075	0.113	0.688
Unimproved	—	—	—	41.1	1.966	0.116	0.608	1.097

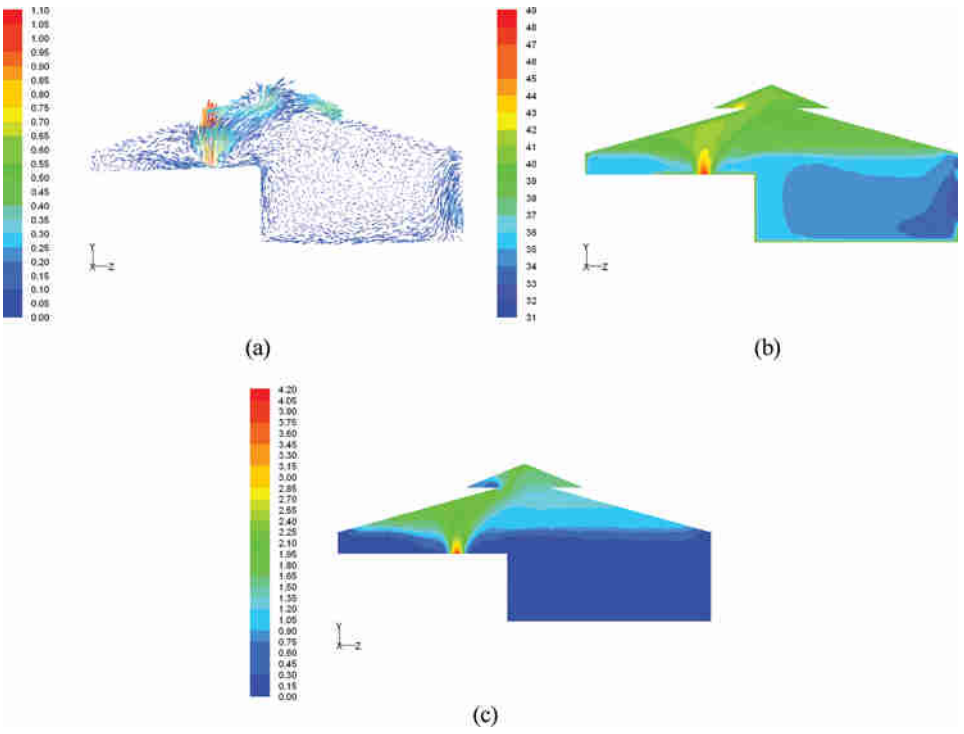

Figure 11. The ventilation improvement as of Case 1 shown for plane $C - C'$: (a) vector of velocity magnitude, (b) contours of temperature, and (c) contours of particle concentrations. (Figure available in color online.)

Results of velocity fields, temperature, and particle concentration contours are shown only at plane $C - C'$ for Case 1, which is the most effective case in this study, as shown in Figures 11a–11c. This is because the patterns of these parameters are in a similar fashion for all four cases. The addition of the ridge vent helped the ventilation of the smoke particles considerably. Most of the particles left the cooperative via the space below the ridge, while a small amount escaped via the opening on the rear side of the smoke rooms (IO6). In this case, IO3 and IO4 acted as inlets of ambient air that caused the flow inside the workplace and slightly increased the ventilation through the ridge vent. The contour plot of aerosol concentration in Figure 11c indicates distinguished layers between the high concentration of the top part and the low concentration of the bottom part.

Conclusion

Results between measurements and simulations show that areas of high velocity, temperature, and particle concentration are located above the ventilating lid exits and below the roof. These locations are the inlets of the system domain where smoke particles enter from sources in the workplace area. Air and smoke from the ventilating lids generally flow upward to the roof of the cooperative and then spread in all directions. Part of the air and smoke is vented out of the workplace area, while the remaining circulates inside. A significant amount causes contamination of the air due to smoke particles, which can become hazardous to workers' health.

Particle concentration remains high in areas above the ceiling and is reduced along the elevation in a downward direction. Though the concentration in the workplace area is not extremely high, improvement of ventilation of smoke particles is necessary. This is because when all of the smoke rooms are used for RSS production, the concentration of aerosol particles will become much higher and more harmful for workers. Modification of the roof to include the ridge vent will considerably improve the ventilation, which will result in a significant decrease of aerosol particle concentration inside the factory.

References

Chomanee, J., S. Tekasakul, P. Tekasakul, M. Furuuchi, and Y. Otani. 2009. Effects of moisture content and burning period on concentration of smoke particles and particle-bound polycyclic aromatic hydrocarbons from rubber-wood combustion. *Aerosol and Air Quality Research* 9: 404–411.

Choosong, T., M. Furuuchi, P. Tekasakul, S. Tekasakul, J. Chomanee, T. Jinno, M. Hata, and Y. Otani. 2007. Working environment in a rubber sheet smoking factory polluted by smoke from biomass fuel burning and health influences to worker. *Journal of Ecotechnology Research* 13: 91–96.

Choosong, T, J. Chomanee, P. Tekasakul, S. Tekasakul, Y. Otani, M. Hata, and M. Furuuchi. 2010. Workplace environment and personal exposure of PM and PAHs to workers in natural rubber sheet factories contaminated by wood burning smoke. *Aerosol and Air Quality Research* 10: 8–21.

Chow, W. K., and R. Yin. 2006. Smoke movement in a compartmental fire. *Journal of Fire Sciences* 24: 445–463.

Doo-ngam, N., P. Rattanadecho, and W. Klinklai. 2007. Microwave pre-heating of natural rubber. *Songklanakarin Journal of Science and Technology* 29: 1599–1608.

Einberg, G. 2005. Air diffusion and solid contaminant behaviour in room ventilation—A CFD based integrated approach. Doctoral thesis, Royal Institute of Technology, Stockholm, Sweden.

Haider, A., and O. Levenspiel. 1989. Drag coefficient and terminal velocity of spherical and nonspherical particles. *Powder Technology* 58: 63–70.

Hubert, M., H. Kalman, T. Kravchik, and U. German. 2004. Aerosol sampling efficiency in a model room. *Particulate Science and Technology* 22: 151–168.

Hussein, T., H. Korhonen, E. Herrmann, K. Hämeri, K. E. J. Lehtinen, and M. Kulmala. 2005. Emission rates due to indoor activities: Indoor aerosol model development, evaluation, and applications. *Aerosol Science & Technology* 39: 1111–1127.

Kalasee, W., S. Tekasakul, Y. Otani, and P. Tekasakul. 2003. Characteristics of soot particles produced from rubberwood combustion. *Proceedings of the Second Asian Particle Technology Symposium*, 103–108, Penang, Malaysia.

Kanaoka, C., M. Furuuchi, T. Myojo, J. Inaba, and K. Ohmata. 2006. Numerical investigation of flow and dust concentration distributions in the work area of a mountain tunnel currently under construction. *Aerosol and Air Quality Research* 6: 231–246.

Patankar, S. V. 1980. *Numerical Heat Transfer and Fluid Flow*. New York: Hemisphere.

Promtong, M., and P. Tekasakul. 2007. CFD study of flow in natural rubber smoking-room: I. validation with the present smoking-room. *Applied Thermal Engineering* 27: 2113–2121.

Sohn, M. D., M. G. Apte, R. G. Sextro, and A. C. K. Lai. 2007. Predicting size-resolved particle behaviour in multizone buildings. *Atmospheric Environment* 41: 1473–1482.

Tekasakul, P., and M. Promtong. 2008. Energy efficiency enhancement of natural rubber smoking process by flow improvement using a CFD technique. *Applied Energy* 85: 878–895.

Tian, Z. F., J. Y. Tu, and G. H. Yeoh. 2007. CFD studies of indoor airflow and contaminant particle transportation. *Particulate Science and Technology* 25: 555–570.

Zhang, Z., and Q. Chen. 2006. Experimental measurements and numerical simulations of particle transport and distribution in ventilated rooms. *Atmospheric Environment* 40: 3396–3408.